JACS
JOURNAL OF THE AMERICAN CHEMICAL SOCIETY
pubs.acs.org/JACS
Communication

5′-Phosphorylation Strengthens Sticky-End Cohesions

Zhe Li, Mengxi Zheng, Longfei Liu, Nadrian C. Seeman,* and Chengde Mao*

Cite This: J. Am. Chem. Soc. 2021, 143, 14987−14991
Read Online

ABSTRACT: Sticky-end cohesion plays a critical role in molecular biology and nucleic acid nanotechnology. Although free energy calculations and molecular mechanics can predict these interactions, chemical modification would compromise such predictions. Herein, we have used rationally designed 3D DNA crystals as a tool to experimentally investigate the modulation of 5′-phosphorylation on sticky-end cohesions. We have found that 5′-phosphorylation strengthens the sticky-end cohesion: in a DNA crystal self-assembled exclusively via sticky-end cohesions, 5′-phosphorylation not only promotes the crystallization process, in general, but also accelerates the crystal growth along designed directions. Such a finding allows the fine-tuning of DNA crystallization kinetics and the control of DNA crystal morphology. It also suggests a potential difference in self-assembly kinetics between natural DNA (with 5′-phosphorylation) and synthetic DNA (without 5′-phosphorylation).

Sticky ends are overhung, unpaired nucleotides at DNA duplex ends. Hybridization between sticky ends associates two DNA duplexes together. Sticky-end cohesion not only is a critical foundation for recombinant DNA technology but also acts as one essential pillar for the fast-growing field of structural DNA nanotechnology, where it functions as a programmable DNA−DNA interface during the self-assembly of DNA structural motifs.[1,2] For both genetic engineering and DNA nanotechnology, the strength of sticky-end cohesion is an important parameter. The interaction should be cautiously chosen in an appropriate window so that correct DNA self-assembly can happen, and applications such as DNA computing can be enabled.[3,4] Though previous researchers have used free energy calculations to predict the strength of sticky-end cohesion,[5,6] the results are compromised for subtle changes in the DNA such as chemical modifications. The free energy difference before and after such modifications can be on the same scale of calculation errors. Additionally, computational methods always need to define and verify new parameters to work for custom chemically modified DNA. In this paper, we have established an experimental, qualitative approach to study sticky-end cohesion. It is based on rationally designed 3D DNA triangle crystals, whose self-assembly process is solely driven by sticky-end cohesion.[7,8] By observing the changes of crystallization kinetics and crystal morphology, we are able to inspect how 5′-phosphorylation modulates sticky-end cohesion.

A rationally designed DNA crystal was assembled from DNA tensegrity triangle motifs in 2009 (Figure 1a).[7] In this crystal, one DNA triangle motif connects with its neighboring motifs along the three edges by sticky-end cohesion and extends into a 3D, macroscopic crystal of rhombohedral symmetry. As revealed by X-ray crystallography, all the crystal contacts among triangle motifs are formed via sticky-end cohesion. Therefore, the crystallization kinetics is sensitively dependent on the strength of sticky-end cohesion. Experimental characterization of the crystallization kinetics of DNA triangle crystals also reveals the strength of the sticky-end cohesion.

We focused on the modulation of 5′-phosphorylation on sticky-end cohesion (Figure 1b). 5′-Phosphate often exists in natural DNAs, while it is missing in synthetic DNAs. As DNA materials can be generated by biological mass production,[9,10] it is necessary to understand how 5′-phosphorylation affects DNA self-assembly. For tile-based DNA self-assembly, it is also an important question how sticky-end cohesion is altered by 5′-phosphorylation. Though our previous study shows that 5′-phosphorylation can increase the X-ray diffraction resolution of DNA crystals and do not change the DNA crystal structure (Figure S1),[11] there is no report about the self-assembly process itself. From experimental results, we surprisingly found that 5′-phosphorylation can promote both DNA crystal nucleation and growth (Figure 1c), which indicates that sticky-end cohesion is strengthened by phosphorylation.

The self-assembly of DNA crystal was conducted according to a previously reported hanging drop method.[12] To compare the effect of phosphorylation in parallel, DNA triangles with different phosphorylation sites were assembled under identical conditions. A series of reservoir buffers with different ionic strength were used to explore the solubility boundary of the crystallization diagrams.

5′-Phosphorylation was observed to substantially promote the crystallization of DNA tensegrity triangles. We first tested the crystallization of symmetric, 4-turn DNA triangle ($s\Delta^{4T}$) motif, which has 4 helical turns of DNA duplex as each triangle edge (Figure S2).[13] Different phosphorylation combinations at the sticky ends were screened: no phosphorylation (L+M+S),

Received: July 13, 2021
Published: September 13, 2021

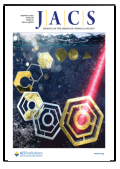

https://doi.org/10.1021/jacs.1c07279
J. Am. Chem. Soc. 2021, 143, 14987−14991

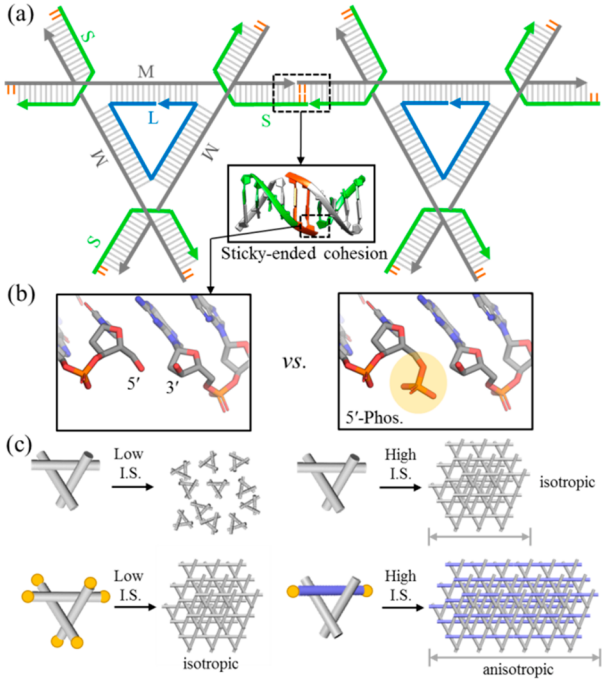

Figure 1. DNA tensegrity triangle crystals as an experimental tool to study 5′-phosphorylation-modulated sticky-end cohesion. (a) Scheme of the crystal contact between two DNA triangle motifs in the crystal. The sticky-end cohesion is boxed and shown in a 3D model. Symmetric 4-turn DNA triangle ($s\Delta^{4T}$) motif is used for demonstration. (b) A putative atomic model of 5′-phosphorylation of the sticky ends. The 5′ phosphate of interest is highlighted by a light yellow oval. (c) Scheme of DNA crystal self-assembly modulated by 5′-phosphorylation. The yellow circles represent 5′-phosphorylation. Phosphorylation promotes both DNA crystal nucleation and growth. I.S.: ionic strength. Phos.: phosphate.

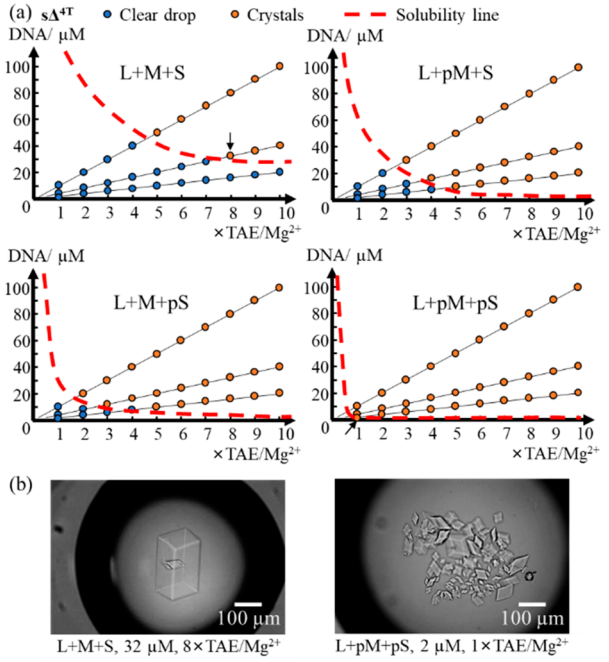

Figure 2. 5′-Phosphorylation promoted the nucleation of DNA $s\Delta^{4T}$ crystals. (a) Crystallization diagram of DNA $s\Delta^{4T}$ crystals in TAE/Mg^{2+} buffer. L, M, and S are strands illustrated in Figure 1a. Prefix "p": 5′-phosphorylated. Crystallizations were set up for 18 days. DNA and buffer concentrations were estimated from the initial drop contents and the reservoir buffer concentrations. The red, dashed solubility lines are sketched to discriminate the crystallization states. (b) Optical images of two representative crystallization drops arrowed point in (a).

phosphorylation on only M strand (L+pM+S), phosphorylation on only S strand (L+M+pS) and phosphorylation on both M and S strands (L+pM+pS). p before any strand name (L, M, or S) indicates phosphorylation of that strand. The results of the screening were presented as crystallization diagrams (Figure 2a), and optical images of DNA crystals were shown in Figure 2b and Figure S3. Solubility lines were sketched as the separations between clear drops and drops with crystals. A trend appeared. With 5′-phosphorylated strands, the solubility line moved toward low concentrations of DNA motif and reservoir buffer. After phosphorylation of both M and S strands, the crystallization can happen at 1/16 DNA concentration and 1/8 lower buffer concentration, respectively. Similar modulation results were also observed for 2-turn and 3-turn DNA triangle ($s\Delta^{2T}$, $s\Delta^{3T}$) crystals (Figure S4). For example, $s\Delta^{2T}$ without 5′-phosphoryaltion remained completely soluble when the reservoir buffer concentration was lower than 10×TAE/Mg^{2+}, while 5′-phosphorylated $s\Delta^{2T}$ crystallize when the reservoir buffer was only 3×TAE/Mg^{2+}.

Based on the observation of accelerated DNA crystallization kinetics, we proposed that 5′-phosphorylation would strengthen sticky-end cohesion. This hypothesis was further proved by the observation that phosphorylation promoted crystal growth in specific directions, thus modulating crystal morphology. An asymmetric 4-turn DNA triangle ($a\Delta^{4T}$) was designed to have three different pairs of sticky ends, GG/CC, GT/AC, and GA/TC, along its three component helices, respectively (Figure 3a). Thus, interactions along the three crystallographic axes could be modulated independently by phosphorylation. The effects of 5′-phosphorylation on $a\Delta^{4T}$ crystallization were summarized in Figure 3b (and Figure S5). (*i*) Without any phosphorylation, $a\Delta^{4T}$ assembled into near isotropic, plate-shaped crystals. (*ii*) When only one pair of sticky ends was phosphorylated, the size along one dimension of the crystals increased relative to the sizes of the other two dimensions. Phosphorylation of the blue sticky end (GA/TC) thickened crystal plates and phosphorylation of either the green (GG/CC) or the orange sticky end (GT/AC) resulted in elongated, plate-shaped crystals. (*iii*) Simultaneous phosphorylation of two of the three pairs of sticky ends increased the sizes along two of the three crystallographic dimensions. For example, the phosphorylation of both GG/CC (green) and GA/TC (blue) resulted in longer and thicker crystal plates. (*iv*) Phosphorylation of all three pairs of sticky ends returned to the original crystal morphology. We further verified the correspondence between the sticky ends identity and the crystal dimensions by both macro-seeding (Figure S6) and numerical fitting (Figure S7). Both results were consistent with our interpretation, and we concluded that 5′-phosphorylation promoted the crystal growth rates along GG/CC (green) and GT/AC (orange) sticky ends by 3.3 and 4.5 times, respectively (Figure S7). To achieve finer tuning of crystal morphology, we phosphorylated only one strand at a time, which generated in a finer, 6-step morphology evolution (Figure S8). The growth rate along the sticky-end direction with only one strand phosphorylated was faster than nonphosphorylated sticky ends, but slower than sticky ends with both stranded phosphorylated. For a given strand, if a mixture of phosphorylated and nonphosphorylated

https://doi.org/10.1021/jacs.1c07279
J. Am. Chem. Soc. 2021, 143, 14987−14991

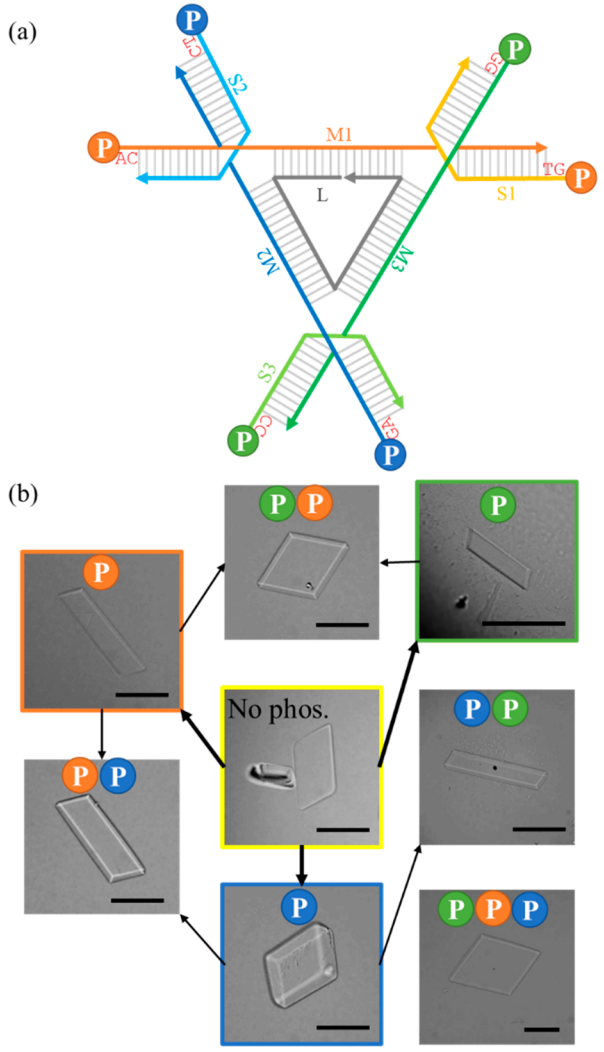

Figure 3. Controlled morphology evolution of asymmetric aΔ^{4T} DNA crystals via 5′-phosphorylation. (a) Scheme of aΔ^{4T} design including the sequences of the three pairs of sticky ends. Circled "P": 5′-phosphorylation. The circle colors match the colors of the continuous strands of the triangle edges. (b) Optical images of aΔ^{4T} DNA crystals with different combinations of 5′-phosphorylation on sticky-ends. The colored circles on the image correspond to the phosphorylated sticky ends in (a). One dimension of the crystal morphology elongates at each stage of evolution. Scale bars: 100 μm.

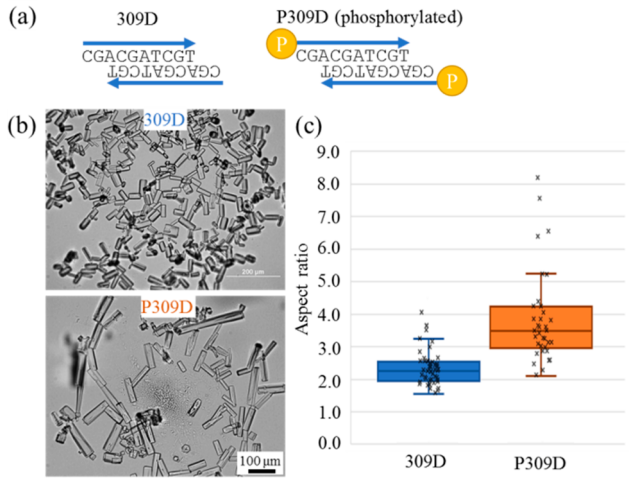

Figure 4. Crystallization of DNA decamer duplex (309D) via sticky-end cohesion. (a) Scheme of the DNA duplexes. (b) Optical images of 309D and P309D crystals. (c) Box plot of the aspect ratios of the rod-shaped crystals (from 100 crystals of 309D and 70 crystals of P309D). All the data points were represented as small crosses. The upper line, the top, middle and bottom line of the box, the lower line represents the upper extreme, upper quartile, median, lower quartile, and lower extreme of the data set, respectively. The data points beyond the range are outliners.

DNAs are used, the crystal growth along that direction positively correlated with the relative percentage of the phosphorylated DNA for this this strand (Figure S9).

Is such phosphorylation-enhanced crystal growth a general phenomenon or specific to the tensegrity triangle? To answer this question, we tested how 5′-phosphorylation affected the crystallization of another previously reported DNA crystal with sticky-end cohesion.[14] The crystal was assembled from a DNA decamer, CGACGATCGT. The DNA first formed an 8-base pair (bp)-long duplex with a CG sticky end at either end. Via axial sticky-end cohesion, the DNA duplex formed infinite, continuous duplexes, which orientated themselves in parallel into crystals. Crystals preferentially grew in the duplex direction and had a rod shape. In all crystallization conditions, phosphorylated DNA showed stronger intermolecular interactions than nonphosphorylated DNA (Figure 4a, Figure S10). In the same buffer where both DNAs formed crystals, crystals of phosphorylated DNA exhibited a higher aspect ratio (3.8 ± 1.4) than that of nonphosphorylated DNA (2.3 ± 0.5) (Figures 4b and 4c). It was consistent with the notion that 5′-phosphorylation enhanced the sticky-end cohesion and promoted the crystal growth along the duplex orientation.

Despite the success in the duplex crystal, another crystal designed from DNA Holliday junctions didn't crystallize well after phosphorylation, even in the same buffer (Figure S11).[15] Likely, the crystal contacts were altered in the presence of 5′-phosphate. From this perspective, the DNA tensegrity triangle crystals represent the best crystal model system to study sticky-end cohesion, where all the crystal contacts are predictable, specific, robust, and resistant to change after chemical modifications.

There is a correlation between free energy calculations and our experimental observations for nonphosphorylated DNA molecules. For the original crystal without phosphorylation, the free energy calculation results from the NUPACK server (http://www.nupack.org/)[16] was qualitatively consistent with our observation of the crystal morphology (Figure S12). To predict DNA with 5′-phosphorylation, we were not able to find available theoretical methods. There are no DNA thermodynamic parameters set up for phosphorylated DNA. As to molecular mechanics, the parameters for 5′ terminal phosphate in DNA were not present in any current force fields including AMBER, CHARMM, etc., to the best of our knowledge.[17,18] Our study represents experimental evidence that 5′-phosphorylation can enhance sticky-end cohesion.

In this study, we have established an experimental approach to study sticky-end cohesion, by using rationally designed DNA triangle crystals as a model system. We have found that 5′-phosphorylation at the sticky ends substantially strengthens sticky-end cohesion. Though the mechanism is not clear now, we speculate that 5′ phosphate could form a H-bond with the 3′ hydroxyl group on the neighboring DNA molecule and potentially other interactions (Figures S13 and S14). Future

https://doi.org/10.1021/jacs.1c07279
J. Am. Chem. Soc. 2021, 143, 14987−14991

high-resolution crystallography study will answer this question. Such strengthening can be readily used to fine-tune crystallization behavior and crystal morphologies. For the broad field of structural DNA nanotechnology, our conclusion underlines an important but previously neglected factor when designing DNA nanomaterials: phosphorylated DNA (from restriction digestion, for example) can have faster self-assembly kinetics than nonphosphorylated DNA (from chemical synthesis, for example). Therefore, DNA designs may require specific optimizations when the assembly materials are advanced from synthetic DNA to biologically produced DNA. Apart from the reported 5′-phosphorylation, we may use such an engineered DNA crystal system to investigate the effect of other DNA modifications (e.g., thiolation, biotinylation, fluorophore modifications, and modified bases) on DNA assembly. Such knowledge is an essential consideration when DNA nanodevices are chemically functionalized. While current theoretical models and calculations are deficient to predict our experimental results, we expect such experimental observations to stimulate theoretical studies that can bring us a deeper understanding of the biophysics behind sticky-end cohesion.

■ ASSOCIATED CONTENT

Supporting Information

The Supporting Information is available free of charge at https://pubs.acs.org/doi/10.1021/jacs.1c07279.

Materials and methods, and additional experimental data (PDF)

■ AUTHOR INFORMATION

Corresponding Authors

Nadrian C. Seeman − *Department of Chemistry, New York University, New York, New York 10003, United States;* orcid.org/0000-0002-9680-4649; Email: ned.seeman@nyu.edu

Chengde Mao − *Department of Chemistry, Purdue University, West Lafayette, Indiana 47907, United States;* orcid.org/0000-0001-7516-8666; Email: mao@purdue.edu

Authors

Zhe Li − *Department of Chemistry, Purdue University, West Lafayette, Indiana 47907, United States;* orcid.org/0000-0001-9402-4940

Mengxi Zheng − *Department of Chemistry, Purdue University, West Lafayette, Indiana 47907, United States*

Longfei Liu − *Department of Chemistry, Purdue University, West Lafayette, Indiana 47907, United States;* orcid.org/0000-0002-5760-2964

Complete contact information is available at: https://pubs.acs.org/10.1021/jacs.1c07279

Notes

The authors declare no competing financial interest.

■ ACKNOWLEDGMENTS

This work was supported by NSF (2025187, 2107393, and 2106790), ONR (N000141912596), and DoE (DE-SC0007991).

■ REFERENCES

(1) Seeman, N. C. Nanomaterials based on DNA. *Annu. Rev. Biochem.* **2010**, *79*, 65−87.

(2) Seeman, N. C.; Sleiman, H. F. DNA nanotechnology. *Nat. Rev. Mater.* **2018**, *3*, 17068.

(3) (a) Stahl, E.; Praetorius, F.; de Oliveira Mann, C. C.; Hopfner, K.-P.; Dietz, H. Impact of Heterogeneity and Lattice Bond Strength on DNA Triangle Crystal Growth. *ACS Nano* **2016**, *10* (10), 9156−9164. (b) Simmons, C. R.; Zhang, F.; Birktoft, J. J.; Qi, X.; Han, D.; Liu, Y.; Sha, R.; Abdallah, H. O.; Hernandez, C.; Ohayon, Y. P.; Seeman, N. C.; Yan, H. Construction and structure determination of a three-dimensional DNA crystal. *J. Am. Chem. Soc.* **2016**, *138*, 10047−10054. (c) Zhang, F.; Simmons, C. R.; Gates, J.; Liu, Y.; Yan, H. Self-assembly of a 3D DNA crystal structure with rationally designed six-fold symmetry. *Angew. Chem., Int. Ed.* **2018**, *57*, 12504−12507. (d) Selmi, D. N.; Adamson, R. J.; Attrill, H.; Goddard, A. D.; Gilbert, R. J. C.; Watts, A.; Turberfield, A. J. DNA-templated protein arrays for single-molecule imaging. *Nano Lett.* **2011**, *11*, 657−660. (e) Park, S. Y.; Lytton-Jean, A. K. R.; Lee, B.; Weigand, S.; Schatz, G. C.; Mirkin, C. A. DNA-programmable nanoparticle crystallization. *Nature* **2008**, *451*, 553−556. (f) Nykypanchuk, D.; Maye, M. M.; van der Lelie, D.; Gang, O. DNA-guided crystallization of colloidal nanoparticles. *Nature* **2008**, *451*, 549−552. (g) Zhang, D.; Paukstelis, P. J. Designed DNA crystal habit modifiers. *J. Am. Chem. Soc.* **2017**, *139*, 1782−1785. (h) Ohayon, Y. P.; Hernandez, C.; Chandrasekaran, A. R.; Wang, X.; Abdallah, H. O.; Jong, M. A.; Mohsen, M. G.; Sha, R.; Birktoft, J. J.; Lukeman, P. S.; Chaikin, P. M.; Ginell, S. L.; Mao, C.; Seeman, N. C. Designing Higher Resolution Self-Assembled 3D DNA Crystals via Strand Terminus Modifications. *ACS Nano* **2019**, *13*, 7957−7965.

(4) Evans, C. G.; Winfree, E. DNA Sticky End Design and Assignment for Robust Algorithmic Self-assembly. *DNA 19 Proceedings of the 19th International Conference on DNA Computing and Molecular Programming* **2013**, *8141*, 61−75.

(5) Lucia, J. S., Jr.; Hicks, D. The Thermodynamics of DNA structural motifs. *Annu. Rev. Biophys. Biomol. Struct.* **2004**, *33*, 415−440.

(6) Ban, E.; Picu, C. R. Strength of DNA sticky end links. *Biomacromolecules* **2014**, *15* (1), 143−149.

(7) Zheng, J.; Birktoft, J. J.; Chen, Y.; Wang, T.; Sha, R.; Constantinou, P. E.; Ginell, S. L.; Mao, C.; Seeman, N. C. From molecular to macroscopic via the rational design of a self-assembled 3D DNA crystal. *Nature* **2009**, *461*, 74−77.

(8) Nguyen, N.; Birktoft, J. J.; Sha, R.; Wang, T.; Zheng, J.; Constantinou, P. E.; Ginell, S. L.; Chen, Y.; Mao, C.; Seeman, N. C. The absence of tertiary interactions in a self-assembled DNA crystal structure. *J. Mol. Recognit.* **2012**, *25* (4), 234−237.

(9) Praetorius, F.; Kick, B.; Behler, K. L.; Honemann, M. N.; Weuster-Botz, D.; Dietz, H. Biotechnological mass production of DNA origami. *Nature* **2017**, *552*, 84−87.

(10) Ducani, C.; Kaul, C.; Moche, M.; Shih, W. M.; Högberg, B. Enzymatic production of monoclonal stoichiometric single-stranded DNA oligonucleotides. *Nat. Methods* **2013**, *10*, 647−652.

(11) Sha, R.; Birktoft, J. J.; Nguyen, N.; Chandrasekaran, A. R.; Zheng, J.; Zhao, X.; Mao, C.; Seeman, N. C. Self-assembled DNA crystals: The impact on resolution of 5′-phosphates and the DNA source. *Nano Lett.* **2013**, *13*, 793−797.

(12) Zhao, J.; Zhao, Y.; Li, Z.; Wang, Y.; Sha, R.; Seeman, N. C.; Mao, C. Modulating Self-Assembly of DNA Crystals with Rationally Designed Agents. *Angew. Chem., Int. Ed.* **2018**, *57* (50), 16529−16532.

(13) Li, Z.; Liu, L.; Zheng, M.; Zhao, J.; Seeman, N. C.; Mao, C. Making engineered 3D DNA crystals robust. *J. Am. Chem. Soc.* **2019**, *141*, 15850−15855.

(14) Qiu, H.; Dewan, J. C.; Seeman, N. C. A DNA decamer with a sticky end: the crystal structure of d-CGACGATCGT. *J. Mol. Biol.* **1997**, *261* (4), 881−898.

(15) Venkadesh, S.; Mandal, P. K.; Gautham, N. The sequence d(CGGCGGCCGC) self-assembles into a two dimensional rhombic DNA lattice. *Biochem. Biophys. Res. Commun.* **2011**, *407* (3), 548−551.

(16) Zadeh, J. N.; Steenberg, C. D.; Bois, J. S.; Wolfe, B. R.; Pierce, M. B.; Khan, A. R.; Dirks, R. M.; Pierce, N. A. NUPACK: analysis and design of nucleic acid systems. *J. Comput. Chem.* **2011**, *32*, 170−173.
(17) Zgarbová, M.; Sponer, J.; Otyepka, M.; Cheatham, E. T., III; Galindo-Murillo, R.; Jurecka, P. Refinement of the sugar−phosphate backbone torsion beta for AMBER force fields improves the description of Z-and B-DNA. *J. Chem. Theory Comput.* **2015**, *11* (12), 5723−5736.
(18) Ivan, I.; Dans, P. D.; Noy, A.; Pérez, A.; Faustino, I.; Hospital, A.; Walther, J.; Andrio, P.; Goñi, R.; Balaceanu, A.; Portella, G.; Battistini, F.; Gelpí, J. L.; González, C.; Vendruscolo, M.; Laughton, C. A.; Harris, S. A.; Case, D. A.; Orozco, M. Parmbsc1: a refined force field for DNA simulations. *Nat. Methods* **2016**, *13*, 55−58.

https://doi.org/10.1021/jacs.1c07279
J. Am. Chem. Soc. 2021, 143, 14987−14991